Optical link as an alternative for MRI receive coils: toward a passive approach

Paul Nobre, Gwenael Gaborit, Raphaël Sablong, Nadege Courjal, Florent Behague, Antoine Coste, Miguel Suarez, Lionel Duvillaret, Olivier Beuf

Optical Link as an Alternative for MRI Receive Coils: Toward a Passive Approach

Paul Nobre, Gwenaël Gaborit, Raphaël Sablong, Nadège Courjal, Florent Behague, Antoine Coste, Miguel Suarez, Lionel Duvillaret, and Olivier Beuf

Abstract*—*Objective: **The objective of this work was to propose an alternative solution to NMR signal transmission by replacing the coaxial cables of the receiver radiofrequency (RF) coil in the context of MRI so as to improve safety. Starting from the analysis of previous studies and reports on the topic, the difficulty of supplying power wirelessly to an RF coil was identified. To avoid this difficult task, the development of a passive analog optical link was studied. Methods: In order to quantify the requirements for achieving an analog conversion, the performance of the link was evaluated based on the input NMR signal amplitude and the optical power and compared with that of a galvanic link. Acquisitions were performed on a 7-T preclinical MRI system with a doped saline solution as phantom. A passive and MRI-compatible polarization-state custom-made modulator was tested as well as a commercial Mach–Zehnder interferometer. Results: The conversion was not sensitive enough to keep similar SNRs, but the main source of noise was identified along with parameters for improvement. Optical power emitted by the laser, insertion loss, and full-phase inversion voltage of the modulators were found to be crucial characteristics for the application. These data indicate that custom application devices are required since the frequency, bandwidth, and amplitude of NMR signals are quite different to usual telecommunication signals. Conclusion: An electro-optic modulation and a transmission channel were successfully conceived and tested. Images were reconstructed with some significant SNR drawbacks that are expected to be compensated with an appropriate modulator. Significance: While technical challenges remain, our approach to a two-decades-long problem could solve a major issue of MRI safety by removing the need for supplying on-coil electrical current.**

***Index Terms*—Magnetic resonance imaging, RF MR coil, optical modulation, fibered sensor.**

I. Introduction

COAXIAL cables are widely used for the transmission of analog signals. In the general case of MRI, coaxial cables transmit the signal from the receiver coil to the console for digital signal conversion. Galvanic links such as coaxial cables are also associated with limitations and hazard sources [1] as they can interact with the B_1 transmit magnetic field and induce radiofrequency (RF) burns [2]. When an RF magnetic field is emitted by the body coil, common mode currents can flow along the cable of the receiver coil inducing an electric field in the patient's tissue.

This issue is well known and is generally avoided by using electrical circuits such as cable traps or balun [3]. Nevertheless, such circuits are usually bulky and rigid. Involving arrays of surface coils with many elements, which is the trend in MR coils currently [4], [5], this solution is of significant weight. Moreover, cable traps are so cumbersome that they still would not enable proper insertion of endoluminal coils to the area of interest during most cases of digestive tract exploration [6], [7]. Great efforts have been made to reduce the size and weight of baluns. However the size of the smallest produced baluns still is of the order of the tenths of mm [8], [9], while the optical fiber and modulator considered for endoluminal application are millimeter sized. As demonstrated for the colon wall, endoluminal coils take advantage of the very high spatial resolution achievable due to the high sensitivity of small loop coils at close proximity [10]. It is promising for the staging of colorectal cancers, a type of cancer where the early detection stage has tremendous influence on the survival rate [11]. Such coils still need and deserve a safer way of transmitting the receive MR signal.

Independently of safety concerns, the coaxial cables can have an impact on the integrity of the signal. The residual common mode currents not filtered by cable traps degrade the SNR [2], and the length of the cable makes impedance matching a complex process [12], which creates some additional losses of signal. Furthermore, the interference between cables due to

Manuscript received 19 September 2022; accepted 23 October 2022. Date of publication 4 November 2022; date of current version 21 April 2023. This work was supported by the AURA region and performed within the scope of LabEx PRIMES under Grant ANR-11-LABX-0063. Experiments were performed on the PILoT facility, part of the France Life Imaging infrastructure (ANR-11-INBS-0006). *(Corresponding author: Olivier Beuf.)*

Paul Nobre and Raphaël Sablong are with the Univ Lyon, INSA-Lyon, Université Claude Bernard Lyon 1, CNRS, Inserm, CREATIS UMR 5220, U1294, France.

Gwenaël Gaborit is with the IMEP-LAHC, UMR 5130, University of Savoie, France.

Lionel Duvillaret is with the KAPTEOS, France.

Nadège Courjal, Florent Behague, Antoine Coste, and Miguel Suarez are with the FEMTO-ST Institute, Université Bourgogne Franche-Comté, Besancon, France.

Olivier Beuf is with the Univ Lyon, INSA-Lyon, Université Claude Bernard Lyon 1, CNRS, Inserm, CREATIS UMR 5220, U1294, F-69621 Lyon, 73000 Chambéry, France (e-mail: olivier.beuf@creatis.insa-lyon.fr).

Digital Object Identifier 10.1109/TBME.2022.3217822

mutual inductance of the different channels of an array is also troublesome with a geometric dependency [1].

These are the principal reasons prompting research for alternative solutions to convert and transmit the MR signal. There are several strategies to overcome the need for galvanic connections. The two most promising are wireless and optical transmissions.

A. Wireless Transmission

Wireless transmission of analog or digital signal in the MRI context has been investigated since the early 2000s. As in telecommunications, a clear tendency for digital transmission emerged. In order to be wirelessly transmitted, the digital signal first has to be conditioned. This involves on-coil amplification, digital conversion, and eventually compression depending on the protocol used. The mode of transmission most widely investigated is Wi-Fi technology (GHz domain) [13]. It can be challenging to introduce such a device that is compatible with the environment and requirements of MRI, but studies have shown conclusive transmission of data in the MRI bore as the gradient and RF field were turned off [14], [15].

The optical frequency domain is an alternative that has also been studied, whether infrared (IR) or visible [16]. Compared with Wi-Fi, it has the advantage of less risk of interference but it requires a line of sight [17], not always obvious to conserve.

B. Optical Fiber Transmission

Electro-optical (EO) conversion is a process where an electric signal is used to modulate a laser beam guided in an optical fiber. The laser is controlled either directly with the signal (direct modulation) or by a crystal whose refraction index changes when applied to an electric field (external modulation). The MR system expects an electric signal, and therefore the optical modulation has to be converted back to the electric domain by a photodiode (OE conversion).

In the late 2000s, various teams succeeded in demonstrating the inherent benefit of this method [18], [19], [20]. The structures of the links were embedded amplifiers and laser diodes on coils, coupled with optical fibers. This technique has many advantages: It does not interact with the magnetic field, the diameter of a fiber is in the submillimeter range, and fibers do not interact with each other. The setup used in the aforementioned studies, however, makes use of active components.

C. Wireless Power Supply

Another critical point in the aforementioned techniques lies in the power supply to on-coil components. It is truly challenging to bring power to the coil without cables while guaranteeing the safety of the patient. Three principal possibilities were explored. Non-magnetic batteries: Instead of "sending" energy to the coil, the power supply is also embedded. Lithium polymer batteries with a custom converter have been tested at 1.5 T in several studies [14], [19]. This setup solves the supply problem even for a large number of channels, but at the cost of space (a 6000-mAh 3.7-V battery is $138 \times 58 \times 6$ mm^3), and the impact on image quality, especially at high field, needs to be further inspected. Optical power: The principle is the same as a solar panel, making use of light absorbed by semiconductors (photodiodes) to produce electric currents. This technique has worked well for small amounts of power (tens to hundreds of milliwatts) [21] but it becomes troublesome for larger values. It was successfully implemented to detune receive coils, for instance [22]. Electromagnetic induction: the physical principle is the same as in transformers, where the magnetic flux is used to transport the energy from a primary to a secondary coil. This method has successfully sent tens of Watts [23] in an MRI bore, which would be enough to power 32 channels needing 300 mW [24]. The effect on the patient's specific absorption rate (SAR) and image quality are yet to be estimated, and the positioning of the coil is important to avoid interferences [23].

To solve this issue, some scanner manufacturers have worked on optical transmission with wired power supply. Philips Healthcare, for instance, has developed and marketed a line of scanners with the commercial "dStream" denomination [25], which aims at cancelling the loss of signal inherent to coaxial cables at high frequencies and the clutter of cables in phased array coils. The approach is used to perform AC conversion directly on the coil, before performing an EO conversion. Since the analog–digital converters (ADC) need power supply, there is still a galvanic link, but the signal is carried through optical fibers. This solution addresses part of the problem but is not suited to endoluminal applications, as the supply cable remains voluminous with baluns.

To avoid the issue of the wireless power supply, and to address all the issues of coaxial cables, our approach was to estimate the feasibility of passive optical conversion. In this work, we assessed the experimental settings and conditioning of signals to perform an EO conversion without power supply. The key elements of the transmission chain were examined and analyzed to establish the remaining challenges of a completely passive conversion for a receive-only coil.

II. Theory

Some insights into EO modulation and the origins of noise are required to analyze the performance of an optical link.

A. Considerations on Optical Conversion

To understand the impact of conversions and to design correctly the chain of transmission, with regard to the targeted application, we must inspect each element involved in the process.

For external modulation, three elements interact: a continuous-wave (CW) laser, an EO modulator, and a photodiode. The modulator will be the subject of special focus, as it should be embedded in the coil, while the laser and photodiode will only be studied in view of their impact on the SNR.

The principle of an EO modulator is to modify the properties of the light passing through it. As mentioned in I), in order to reach that objective, an EO crystal is used. When an electric field is applied, its refractive index changes, which modifies the phase of the wave propagating inside [26].

The important characteristics of the crystal are:

-Its EO coefficients r [m/V], which describe the geometric variation of the unit cell of the EO crystal for a given electric field E

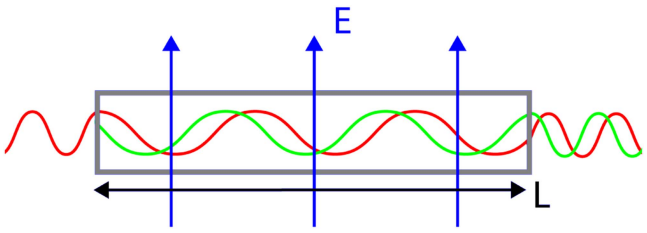

Fig. 1. Light wave propagating through an EO crystal (in blue). The phase shift between the wave entering and exiting is proportional to the distance travelled by the laser beam, the EO coefficients of the crystal, and the intensity of the electric field. Birefringence, used in polarization modulation, leads to a phase shift between the polarization axis (green and red curves).

(order of tens of pm/V, greater value yields more modulation depth). The EO coefficients depend on the material and on the orientation of the optical wave vector travelling through the crystal.

-Its length *L*: The optical phase shift $\Delta\varphi$ [rad] is proportional to the distance travelled by the laser beam in the crystal (Fig. 1).

$$\Delta\varphi \propto E * L * r \tag{1}$$

There is a trade-off, however, with the bandwidth of the modulator due to the length of the electrodes on the crystal [27]: Longer electrodes produce a more sensitive device, but they act as a low-pass filter.

B. Signal and Noise

A major issue of the transmission is to preserve the integrity and quality of the signal. If we look at the sources of noise in the conversion, three prevail [28].

The first source is Johnson noise (or thermal noise). It is generated by the random movements of electrons in leads induced by thermal agitation [29]. The power of the Johnson noise (δP_j) is proportional to the temperature of the resistor *T* in Kelvin, and to the bandwidth Δf of the signal [30]. If we use the same MRI sequence, we can consider the bandwidth constant:

$$\delta Pj\ (T) = 4 * K_b * T * \Delta f \tag{2}$$

with K_b the Boltzmann constant (1380 649 $\times$ 10^{-23} J.K^{-1}).

This type of noise deteriorates every electric signal, and therefore it also contributes to noise in MRI examinations [31].

The second source of noise is associated with the photodiode: the shot noise (or quantum noise) [32]. It represents the probabilistic aspect of light: Instead of an ideal constant-amplitude light beam, photons are distributed following a Poisson law distribution. The same applies to the electric current that is composed of single electrons instead of a continuous current. These variations are described as the power of the shot noise δP_{sn} according to the optical power P_{opt} received.

$$\delta P_{sn}\ (P_{opt}) = 2 * R_{pd} * \eta * q * P_{opt} * \Delta f \tag{3}$$

R_{pd} [Ω] is the resistance load of the photodiode, η [A/W] is the photodiode efficiency, and *q* [C] is the charge of the electron.

The third noise source originates in the laser diode; it is the relative intensity noise (RIN). It describes the unwanted fluctuation of the light emitted, as photons can be spontaneously emitted instead of being willingly amplified. The RIN varies with the optical power according to a square law relation [30]:

$$\delta P_{RIN} = R_{pd} * \left(\eta * P_{opt} * 10^{RIN}\right)^2 * \Delta f \tag{4}$$

with the value RIN in [dB.Hz^{-1}], a characteristic of a given laser diode.

The sum of the noise contribution of the conversion according to the optical power is as follows:

$$\delta P_{noise} \propto \delta Pj + \beta P_{opt} + \gamma P_{opt}^2 \tag{5}$$

with δPj the thermal noise factor, β the shot noise factor, and γ the RIN factor. The amplitude of the useful signal increases with P_{opt} and with $1/V_\pi$, which is the voltage required for a full-phase inversion of the signal for a given modulator. There is an optimal point of operation for optical power according to equation (6):

$$SNR \propto \frac{P_{opt}}{V\pi\left(\delta Pj + \beta P_{opt} + \gamma P_{opt}^2\right)} \tag{6}$$

This consideration on noise must be put in perspective with the NMR signal amplitude. The amplitude of the NMR signal depends on a wide set of parameters, the most important being the volume V considered, the static field B0, the flip angle θ and the receive coil size and geometry.

Quantitative description of the electromotive force (Emf) through the reprocity principle has been vastly studied by D. Hoult and other authors [33] The principle of reciprocity states that the Emf induced in the receive coil is proportional to the magnetic field it would create with a unit current *I* flowing through it, and the equation can be derived as follow :

$$Emf \approx \omega_l * (B_{1xy}/I) * M * V * cos(\omega l * t) \tag{7}$$

with ω_l the larmor angular frequency, B_{1xy} the transverse magnetic field generated by the coil in the volume *V* when being applied unit current *I* and *M* the macroscopic magnetization M in the volume.

The equation (7) shows that the amplitude of the signal is greatly dependant on hardware, the object of the study and sequence specifications, but a common order of magnitude is the hundreds of microvolt to millivolt [34], [35].

Using the equation (2). for a 50 Ohm receiver at 20 °C, the thermal noise floor is of the order of the tenth of nanovolts for conventional MR bandwidths (order of the tens or hundreds of khz), leading to a dynamic range (DR) of 80 dB (even if 120 dB DR for specific high resolution 3D applications can occur) [36].

III. Material and Methods

Our starting point was the conversion of the unamplified NMR signal, with "off-the-shelf" optical communication devices. The aim was to find the dominant source of noise, to set requirements for the sensitivity of the EO and OE conversions, and to propose leads of improvement.

All the images were acquired on a 7-T preclinical MRI scanner (Bruker, Germany). A quadrature mouse head coil of 23 mm inner diameter was used in reception instead of an endoluminal coil. Compared to this latter, the signal received by the coil is rather uniform with a homogenous phantom. The volume coil

make easier image comparisons compared to small diameter surface coil with rapid decrease of SNR with distance from the coil. A receive only coil would also require active detuning during B1 transmit period. This task was addressed by our lab by Saniour et al. in a previous work [37]. The system developed based on optical detuning with a circuit associating a photodiode and PIN diode was compared to usual detuning circuits and validated at 3 T. With 38.5 dB isolation and a switching delay inferior to 10 µs, proposed circuit was suitable with clinical requirements. This allows focusing on the conservation of the NMR signal. The phantom used consists of a 15-mm-diameter tube filled with doped saline solution (NaCl 5 g/l + NiSo4 1.25 g/l). The sequence used throughout this study was a T1 Flash with a 20° flip angle. The FOV is 40 mm for a 44-kHz receiver bandwidth. In order to separate the transmit signal from the receive signal on this volume coil, the coil was connected to a quadrature hybrid coupler. This device routes on two separate channels the emitting signal (RF pulse) and the receiving NMR signal, to convert the receive signals only. The output of the coupler is connected to the RF port of the EO modulator. The most well-known modulator topology is the Mach–Zehnder modulator (MZM), it makes use of the phase shift to modulate the amplitude of the light. The incoming light is split into two arms, one is modulated and the other is unaltered. When the two are recombined, the waves interfere and the resulting power depends on the phase shift [38]. This type of modulator is very popular in telecommunications because the voltage required for a full-phase inversion can be very low [27], making it a highly sensitive device. However, it requires a bias voltage, which adds a galvanic connection. Moreover the device is not stable with temperature because the refractive index of the crystal also varies according to that parameter [39].

A second option is polarization state modulation (PSM). Instead of modulating the phase, we modulate the polarization of light. An EO crystal is also used, but its refractive indexes vary with different coefficients according to the axis of polarization [40]. The PSM requires no voltage bias and is independent of the temperature, because the two axes have the same thermal variations. The PSM used has however more signal insertion loss.

First a commercial LN82S-FC MZM modulator (Thorlabs) was used. A second PSM modulator developed and built at the FemtoST lab in Besancon (France) was employed. It embeds a 12-mm-long crystal and the packaging is non-magnetic. The modulators were kept outside the bore during this study, because of the magnetic package of the MZM and so as to keep the PSM in the same conditions as the MZM.

The optical ports of the modulator are connected to an optoelectronic unit (EoSense, Kapteos, France), which is an instrumentation device including the laser source (AA1401, G&H, Germany) delivered to the modulator, and the photo diode (G9801, Hamamatsu, Japan) receiving its output. The electrical output of the EoSense is connected to the usual preamplifier of the MRI system to be digitalized and reconstructed (Fig. 2).

The acquisitions are performed alternatively with galvanic cables (path A) and optical conversion (path B) to have a quantitative reference of SNR. The conversions performed with the MZM and with the PSM are labelled B1 and B2 respectively.

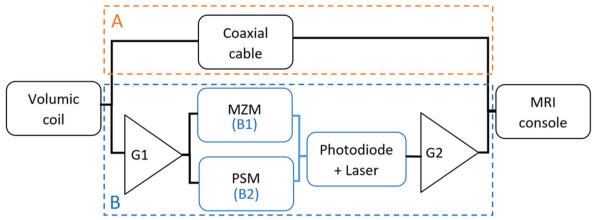

Fig. 2. Both chains of transmission of the NMR signal. The two paths of acquisition are performed alternatively for comparison. The EO modulator is outside the MRI bore because the packaging of the device is not MRI compatible.

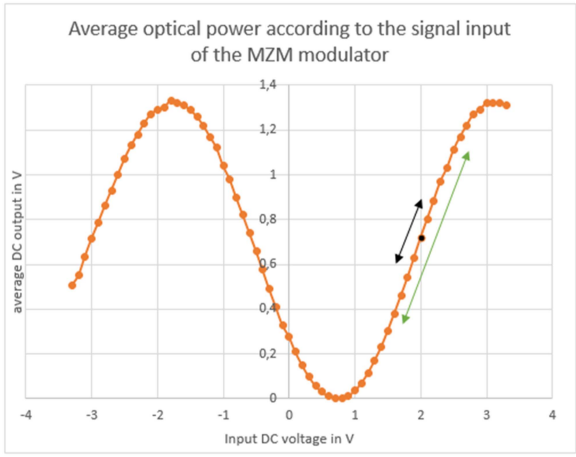

Fig. 3. Operating curve of the MZM modulator. The arrows show the range of operation based on a small-amplitude signal (black) and larger-amplitude signal (green). The DC power output values are measured after an amplification step.

A spectrum analyzer (Agilent, USA) is used to monitor the amplitude of the signals fed to the MRI console. The device and MR sequence are trigged by an external waveform generator to visualize the power density spectrum in the time domain of echo signals. Transmission paths A and B use the same length of coaxial cable in order to have the same loss in both cases.

One of the goals of this study was to set the required modulation efficiency for the OE conversion to match the dynamic range of the coaxial transmission. Fig. 3 shows the measured operating curve of the MZM. The voltage bias sets the operating point in the center of the linear part of the sine wave (in this case at 2 V on the abscissa). A greater sensitivity here means a steeper slope. However, if the input is amplified (like indicated by the green arrow), it behaves like a more sensitive component. Therefore, the first experiment was conducted to amplify gradually the RF signal in order to define the specifications for the modulator.

The amplification between the coil and the modulator is between 0 and 40 dB with 10-dB steps. We used two amplifiers (ZX60-33LN, Microcircuit, USA) of 20-dB gain with a noise factor of 0.9 dB at 300 MHz, and one of 30 dB with 1.4 dB noise factor. A different set of 10-dB attenuators were placed after the amplifier to reach lower values. To make sure that the MRI dynamic amplifier has enough gain, an amplifier was also connected between the photodiode and the MRI preamplifier, ranging from 0 to 30 dB in 10-dB steps. This configuration is described in Fig. 2.

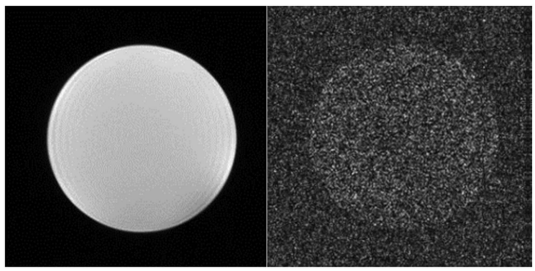

Fig. 4. Comparison of images without (reference) and with EO conversion in configuration B1. The SNR in the reference image is 98 (left) and drops close to 2.5 (right) after direct EO conversion.

Secondly, we mentioned the importance of optical power in the noise added by the conversion. In addition to a parametric study of the sensitivity, a study of the SNR in relation to the optical power was conducted, The SNR is deduced from the ratio of the mean signal in the center of the picture, and the standard deviation of the signal in the corners. The laser used is programmed to function at four different powers, ranging from 6.5 to 35 mW. Because of the attenuation of the modulator, however, the average power received by the photodiode is between 1 and 7 mW.

IV. Results

The results of the unamplified conversion of the NMR signal compared to a reference are depicted in Fig. 4.

Without proper conditioning of the signal, the image is recognizable but drastically deteriorated.

A. Amplification

The visualized signal on the spectrum analyzer reached the maximum value of −60 dBm. With a noise floor close to −130 dBm according to equation (2), the following results are to be considered for maximum DR of 70 dB. The imaging sequence was repeated with different amplification gains ranging from 0 to 40 dB (G1) before the conversion and from 0 to 30 dB (G2) after conversion. The images and SNR are shown in Fig. 5. The different lines correspond to variable G1 values and the columns to variable G2 values. The images in the mosaic were obtained using the configuration B1, the image at the bottom were acquired using configuration A and B2 (G1 = 40 dB) respectively. The SNR is given in the corner or each image.

The polarization state modulator was used in the same configuration as the MZM, with a 7-dB lower signal magnitude witnessed on the spectrum analyzer due to larger insertion loss and higher V_π. By amplifying the input signal up to 70 dB, we found that image SNR reaches a plateau before dropping, because the signal is clipped by the digital converter.

B. Optical Power

To identify the dominating source of noise, we proceeded to an optical power parametric test. Fig. 7 represents the SNR in relation to the optical power emitted by the laser source.

The SNR increases along with the optical power. We could not reach the stage where the SNR would stagnate or decrease.

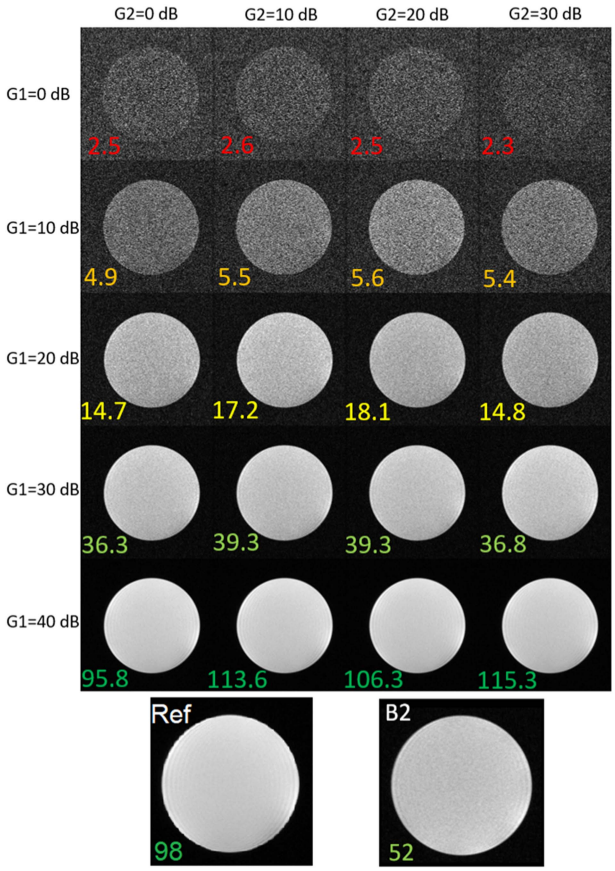

Fig. 5. Series of images acquired with various gains G1 and G2. The SNR value is unaltered by conversion with sufficient prior amplification. All images obtained with configuration B were acquired with 35 mW of optical power. The image with B2 configuration (PSM) was acquired with a signal amplification gain of 40 dB before the conversion.

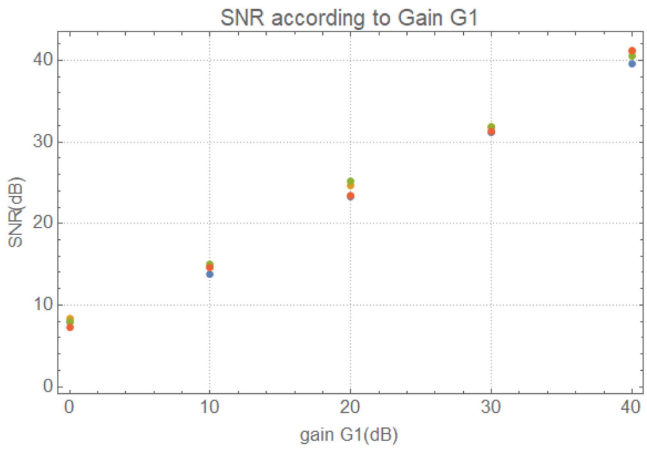

Fig. 6. Graph displaying the SNR as a function of amplifier gain G1 for different values of amplifier gain G2 (orange, blue, green, yellow).

V. Discussion

A. Analysis of Results

Fig. 5 shows that the signal's SNR can be recovered after the EO and OE conversions with appropriate amplification. The 40-dB gain G1 configuration reaches a similar SNR value. Fig. 6 shows however that the SNR gain scales linearly with G1, and

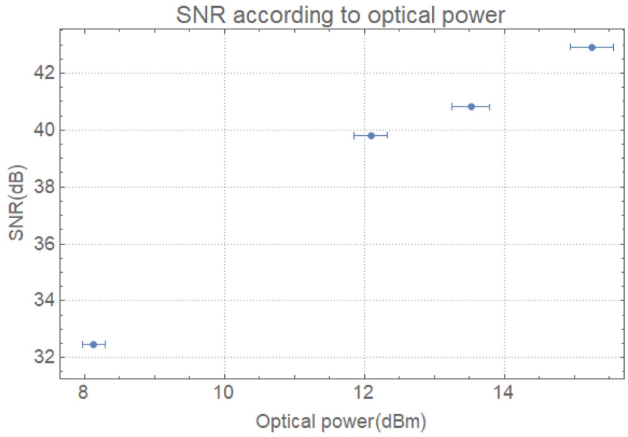

Fig. 7. SNR increases with the optical power. The power displayed on the abscissa is the power emitted by the laser.

that the gain G2 had no impact, as the MRI dynamic amplifier compensated for it.

The reason for the lower signal obtained with the PSM is the higher V_π and that the polarizing (PZ) fiber used allows less light to pass through than the MZM. This directly affects the SNR, as mentioned in Section IV.b. However, the absence of bias voltage still makes the solution worth considering if the prior signal amplification can be avoided.

The temperature stability of the MZM was a recurring issue during the experiment. Despite the stabilized environment of the MRI room, the operating point of the device changed substantially during the period of use, requiring several manual adjustments of bias voltage.

Fig. 7 shows that the optical power is a promising first step for recovering the SNR to bypass the need for amplifiers. We did not reach the point where the SNR stopped increasing, which paves the way for using more powerful lasers. Indeed, as the equation (6) in II) indicate, if the SNR rises with the optical power, it means that the principal coefficient in the denominator relates to the thermal noise δPj. The laser we used had a 35-mW limit with a RIN of -153 dB/Hz. Modern lasers can emit several hundred milliwatts with RINs as low as -168 dB/Hz.

Increasing the optical power is particularly interesting as it is not a trade-off and has no drawback. One could argue that injecting several milliwatts of optical power in a patient could be a hazard source, but it is relatively easy to set an emergency stop for a laser, because the system expects to receive constant average power. The increase also indicates that, in our case, the most important source of noise is thermal noise.

A second axis of improvement is the sensitivity of the modulator. The crystal can be lengthened depending on the target application; a multiplication factor of approximately 4 in sensitivity would lead to the crystal being 48 mm long, which is manageable in most conditions. Secondly, the electrodes are a crucial aspect of the modulator as they set the electric field creating the modulation. Most modulators are designed for telecommunication applications, where the input signal amplitude is higher than NMR signals. Designing custom electrodes on the modulator (with a smaller gap, for instance) to increase the E field locally without increasing the voltage applied is also an avenue worth exploring [38].

Combining the solutions of a more sensitive device with higher optical power could help bridge the 40-dB gap. Other experimental options remain, although they involve longer technological development.

B. Perspectives

An interesting long-term perspective is the use of optical stopband filters to cancel the carrier wave (which represents a major part of the optical power) to only transmit the modulation side bands to the photodiode. The remaining signal could be amplified optically to increase the SNR significantly after the OE conversion.

In order to reduce the issue of dimensions with a longer modulator, a Fabry–Pérot etalon could be used. The length of the modulator is set to the wavelength of interest, and reflective media are added on each side. Then, like a laser cavity, a constructive interference occurs where the light travels the length of the media multiple times before being emitted from the crystal. This allows for lower V_{pi} without expanding the length of the crystal; however, it is a complex design process, especially if it cannot be tuned in real time.

Lastly, if despite the optical power increase the main source of noise remains Johnson noise, the photodiode can be cooled with cryogenic liquids. This reduces the thermal noise significantly (20 dBm difference between 290 °K and 4 °K), and cooling media are common in MRI environments for supraconductive coils. However, it changes the impedance matching [41], and is useless if the RIN becomes the limiting factor.

VI. Conclusion

We believe that passive optical transmission is achievable and represents a breakthrough solution to coaxial cable issues in MRI. Cancelling the need for a wireless power supply enables safe and artifact-free imaging. Further developments in sensitivity are required, however, and many unexplored enhancements remain. Along with the passive optical decoupling system [22] already developed, this could lead to new imaging opportunities, in particular in endoluminal configurations.

References

[1] N. De Zanche et al., "Modular design of receiver coil arrays," *NMR Biomed.*, vol. 21, no. 6, pp. 644–654, Jul. 2008, doi.org/10.1002/nbm.1237

[2] D. M. Peterson et al., "Common mode signal rejection methods for MRI: Reduction of cable shield currents for high static magnetic field systems," *Concepts Magn. Reson.*, vol. 19B, no. 1, pp. 1–8, Oct. 2003.

[3] M. Bilgen et al., "Common mode signal rejection methods for MRI: Reduction of cable shield currents for high static magnetic field systems," *Biomed. Eng.*, vol. 5, no. 1, 2006, Art. no. 3, doi.org/10.1186/1475-925X-5-3

[4] H. Fujita, "New horizons in MR technology: RF coil designs and trends," *Magn. Reson. Med. Sci.*, vol. 6, no. 1, pp. 29–42, 2007, doi.org/10.2463/mrms.6.29

[5] P. B. Roemer et al., "The NMR phased array," *Magn. Reson. Med.*, vol. 16, no. 2, pp. 192–225, Nov. 1990, doi.org/10.1002/mrm.1910160203

[6] H. Dorez et al., "In vivo MRS for the assessment of mouse colon using a dedicated endorectal coil: Initial findings," *NMR Biomed.*, vol. 30, no. 12, 2017, Art. no. e3794, doi.org/10.1002/nbm.3794

[7] Z. K. Shah et al., "Performance comparison of 1.5-T endorectal coil MRI with 3.0-T nonendorectal coil MRI in patients with prostate cancer," *Academic Radiol.*, vol. 22, no. 4, pp. 467–474, Apr. 2015, doi.org/10.1016/j.acra.2014.11.007

[8] J. W. Beenakker et al., "Clinical evaluation of ultra-high-field MRI for three-dimensional visualisation of tumour size in uveal melanoma patients, with direct relevance to treatment planning," *Magn. Reson. Mater. Phys., Biol. Med.*, vol. 29, no. 3, pp. 571–577, Feb. 2016, doi.org/10.1007/s10334-016-0529-4

[9] A. Attaran et al., "2 mm Radius loop antenna and linear active balun for near field measurement of magnetic field in MRI-Conditional testing of medical devices," *IEEE Trans. Electromagn. Compat.*, vol. 62, no. 1, pp. 186–193, Feb. 2020, doi.org/10.1109/TEMC.2019.2896519

[10] A. Kumar et al., "Noise figure limits for circular loop MR coils," *Magn. Reson. Med.*, vol. 61, no. 5, pp. 1201–1209, May 2009, doi.org/10.1002/mrm.21948

[11] M. Arnold et al., "Global patterns and trends in colorectal cancer incidence and mortality," *Gut*, vol. 66, no. 4, pp. 683–691, Apr. 2017, doi.org/10.1136/gutjnl-2015-310912

[12] D. J.-Y. Marion et al., "An alternative tuning approach to enhance NMR signals," *J. Magn. Reson.*, vol. 193, no. 1, pp. 153–157, Jul. 2008, doi: 10.1016/j.jmr.2008.04.026.

[13] L. Nohava et al., "Perspectives in wireless radio frequency coil development for magnetic resonance imaging," *Front. Phys.*, vol. 8, no. 11, 2020, doi.org/10.3389/fphy.2020.00011

[14] K. Aggarwal et al., "A millimeter-wave digital link for wireless MRI," *IEEE Trans. Med. Imag.*, vol. 36, no. 2, pp. 574–583, Feb. 2017, doi.org/10.1109/TMI.2016.2622251

[15] J. Wei et al., "A realization of digital wireless transmission for MRI signals based on 802.11b," *J. Magn. Reson.*, vol. 186, no. 2, pp. 358–663, Jun. 2017, doi.org/10.1016/j.jmr.2007.03.003

[16] G. Konstantinou et al., "Experimental demonstration of an optical wireless MRI compatible PET/SPECT insert front-end," in *Proc. IEEE Nucl. Sci. Symp., Med. Imag. Conf. Room-Temp. Semicond. Detect. Workshop*, 2016, pp. 1–4, doi.org/10.1109/NSSMIC.2016.8069524

[17] A. T. Hussein et al., "10 Gbps mobile visible light communication system employing angle diversity, imaging receivers, and relay nodes," *J. Opt. Commun. Netw.*, vol. 7, no. 8, p. 718, 2015, doi: 10.1364/JOCN.7.000718.

[18] J. Yuan et al., "A 4-channel coil array interconnection by analog direct modulation optical link for 1.5-TMRI," *IEEE Trans. Med. Imag.*, vol. 27, no. 10, pp. 1432–1438, Oct. 2008, doi.org/10.1109/TMI.2008.922186

[19] O. G. Memis et al., "Miniaturized fiber-optic transmission system for MRI signals," *Magn. Reson. Med.*, vol. 59, no. 1, pp. 165–173, Jan. 2008, doi.org/10.1002/mrm.21462

[20] S. Biber et al., "Analog optical transmission of 4 MRI receive channels with high dynamic range over one single optical fiber," in *Proc. 16th Annu. Meeting Int. Soc. for Magn. Reson. Med.*, vol. 1120, 2008, p. 1. [Online]. Available: https://cds.ismrm.org/protected/08MProceedings/PDFfiles/01120.pdf

[21] G. Koste et al., "Magnetic resonance imaging, a commercial application for analog photonics," in *Proc. IEEE Conf. Avionics Fiber-Opt. Photon.*, 2005, pp. 64–65, doi.org/10.1109/AVFOP.2005.1514159.conf

[22] I. Saniour et al., "Active optical-based detuning circuit for receiver endoluminal coil," *Biomed. Phys. Eng. Exp.*, vol. 3, no. 2, 2017, Art. no. 025002, doi.org/10.1088/2057-1976/aa5db0

[23] K. Byron et al., "An RF-Gated wireless power transfer system for wireless MRI receive arrays," *Concepts Magn. Reson. Part B: Magn. Reson. Eng.*, vol. 47, no. 4, 2017, Art. no. e21360, doi.org/10.1002/cmr.b.21360

[24] K. Byron et al., "A wireless power transfer system for MRI scanners," in *Proc. IEEE Wireless Power Transfer Conf. (WPTC)*, 2018, pp. 1–4, doi.org/10.1109/WPT.2018.8639107

[25] C. Possanzini et al., "Scalability and channel independency of the digital broadband dStream architecture," Presented at the ISMRM 19, May 2011. [Online]. Available: https://archive.ismrm.org/2011/1863.html

[26] B. E. Saleh and M. C. Teich, *Fundamentals of Photonics*, 2nd ed. Hoboken, NJ, USA: Wiley, 2007. [Online]. Available: http://lib.ysu.am/disciplines_bk/1e50d8144d6e0c3ffea3ae655684c626.pdf

[27] R. C. Williamson, "Sensitivity–bandwidth product for electro-optic modulators," *Opt. Lett.*, vol. 26, pp. 1362–1363, 2001. [Online]. Available: https://opg.optica.org/ol/abstract.cfm?URI=ol-26-17-1362

[28] E. Ackerman et al., "Low noise figure, wide bandwidth analog optical link," in *Proc. Int. Topical Meeting Microw. Photon.*, 2005, pp. 325–328, doi.org/10.1109/MWP.2005.203604

[29] E. O. Göbel et al., "Some basics," in *Quantum Metrology: Foundation of Units and Measurements*. Germany: Wiley-VCH Verlag GmbH & KGaA, pp. 5–22.

[30] G. Gaborit et al., "A nonperturbative electrooptic sensor for in situ electric discharge characterization," *IEEE Trans. Plasma Sci.*, vol. 41, no. 10, pp. 2851–2857, Oct. 2013, doi.org/10.1109/TPS.2013.2257874

[31] A. Macovski et al., "Noise in MRI," *Magn. Reson. Med.*, vol. 36, no. 3, pp. 494–497, Sep. 1996, doi.org/10.1002/mrm.1910360327

[32] L. N. Binh, *Noises in Optical Communications and Photonic Systems*. Boca Raton, FL, USA: CRC Press, 2016, doi.org/10.1201/9781315372747

[33] D. I. Hoult et al., "The signal-to-noise ratio of the nuclear magnetic resonance experiment," *J. Magn. Reson.*, vol. 24, no. 1, pp. 71–85, Oct. 1976, doi.org/10.1016/0022-2364(76)90233-X

[34] H. Fujita et al., "RF surface receive array coils: The art of an LC circuit: RF surface receive array coils," *J. Magn. Reson. Imag.*, vol. 38, no. 1, pp. 12–25, Jul. 2013, doi.org/10.1002/jmri.24159

[35] L. Nohava, "Lightweight flexible radio frequency coils and optical wireless communication," PhD. Dissertation, 2020. [Online]. Available: https://tel.archives-ouvertes.fr/tel-03141307

[36] R. Behin, J. Bishop, and R. M. Henkelman, "Dynamic range requirements for MRI," *Concepts Magn. Reson. Part B: Magn. Reson. Eng.: An Educ. J.*, vol. 26, no. 1, pp. 28–35, 2005, doi.org/10.1002/cmr.b.20042

[37] I. Saniour et al., "Active optical-based detuning circuit for receiver endoluminal coil," *Biomed. Phys. Eng. Exp.*, vol. 3, no. 2, Feb. 2017, Art. no. 025002, doi.org/10.1088/2057-1976/aa5db0

[38] V. S. Calero et al., "An ultra wideband-high spatial resolution-compact electric field sensor based on Lab-on-Fiber technology," *Sci. Rep.*, vol. 9, pp. 1–10, 2019, doi.org/10.1038/s41598-019-44644-y

[39] N. Courjal et al., "Lithium niobate optical waveguides and microwaveguides," in *Emerging Waveguide Technology*, London, United Kingdom: IntechOpen, 2018, doi: 10.5772/intechopen.76798. [Online]. Available: https://www.intechopen.com/chapters/61408

[40] R. Aydé et al., "Unbiased electro-optic waveguide as a sensitive nuclear magnetic resonance sensor," *IEEE Photon. Technol. Lett.*, vol. 26, no. 12, pp. 1266–1269, Jun. 2014, doi.org/10.1109/LPT.2014.2321099

[41] E. Bardalen et al., "Evaluation of InGaAs/InP photodiode for high-speed operation at 4 K," *Int. J. Metrol. Qual. Eng.*, vol. 9, 2018, Art. no. 13, doi.org/10.1051/ijmqe/2018015